Electronic Supporting information for

Trace tungsten and iron-doped nickel hydroxide nanosheets for an efficient oxygen evolution reaction

Chun Li, Peng Tian**, Hongchang Pang, Weitao Gong, Junwei Ye, Guiling Ning*

State Key Laboratory of Fine Chemicals, School of Chemical Engineering, Dalian University of Technology, Dalian, 116024, China

*Corresponding author. E-mail address: ninggl@dlut.edu.cn .

**Corresponding author. E-mail address: tianpeng@dlut.edu.cn

CAPTIONS

Calculation

Equation S(1) XRD Williamsone-Hall methods

We could get the information about lattice strain and crystalline size based on Williamson–Hall equation through the full width at half maximum (FWHM) of the XRD peak. The W-H equation is (1),

$$\frac{\beta_{hkl} cos\theta}{\lambda} = \frac{k\lambda}{D} + 4\varepsilon sin\theta \quad (1)$$

where D is particle size in nanometer, ε is the strain component without dimensionless, k is a constant equal to 0.94, λ is wavelength of radiation (1.54056 A^o for Cu Kα radiation), β_{hkl} is diffraction peak width at half-maximum intensity, and θ is diffraction angle. By plotting β_{hkl}cosθ versus 4sinθ, we provides more of the crystal structure details, such as the slope and y-intersect of the fitted line represent strain and particle size parameter, respectively.

Equation S(2) To measure electrochemical capacitance, the potential was swept between 0.28 and 0.38 V versus Hg/HgO at ten different scan rates (10, 20, 30, 40, 50, 60, 70, 80, 90 and 100), as shown in Figure S18. The measured capacitive currents are plotted as a function of scan rate and the linear slope is equivalent to twice of the C_{dl}. $Ni(Fe)O_xH_y$ have been determined with an areal capacitance of ~80 μF cm^{-2} in the charged state. The specific capacitances for Carbon Clothes, Ni LDH, $Fe_{0.03}$-Ni LDH, $Fe_{0.03}W_{0.03}$-Ni LDH and $Fe_{0.03}W_{0.03}$-Ni LDH^B are determined as 1.8, 1.9, 1.5, 1.7 and 2.9 mF cm^{-2}, respectively. ECSA is calculated as follows:

$$A_{ECSA} = \frac{C_{dl}^{sample}}{80\mu F^{NiO}} \quad (2)$$

Equation S(3) For temperature-dependent measurements, the kinetics of the OER are increased at elevated temperatures from 20°C to 60°C, reflecting the temperature dependence of the chemical rate constant, which is approximately proportional to exp(-ΔH*/kT). The Arrhenius equation is (3),

$$\frac{\partial(\log i_k)}{\partial(1/T)} = \frac{-\Delta H^*}{2.3R} \ (\eta = 300mV) \tag{3}$$

where ΔH* is the apparent enthalpy of activation (here after simply termed as the activation energy), i_k is the kinetic current at η = 300 mV, T is the temperature, and R is the universal gas constant.

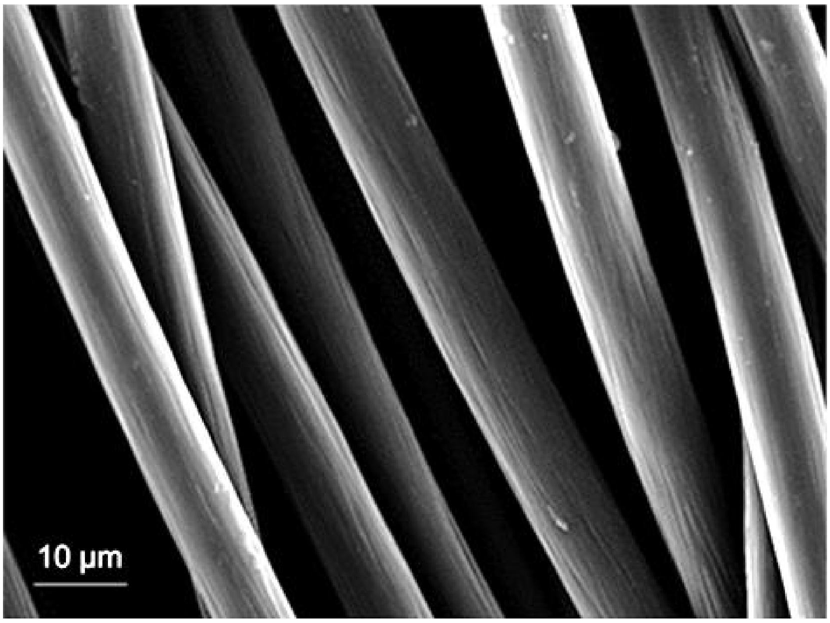

Fig. S1 SEM image of carbon fiber clothes

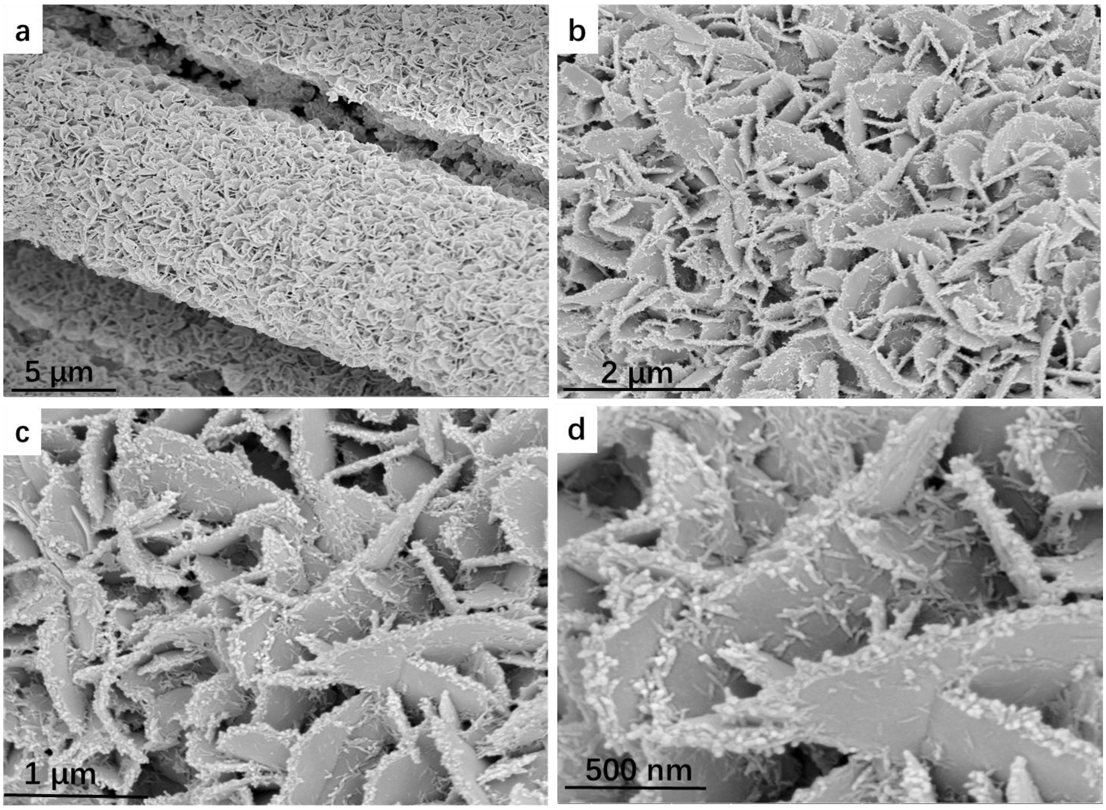

Fig. S2 SEM images of $Fe_{0.03}W_{0.03}$-Ni LDH samples

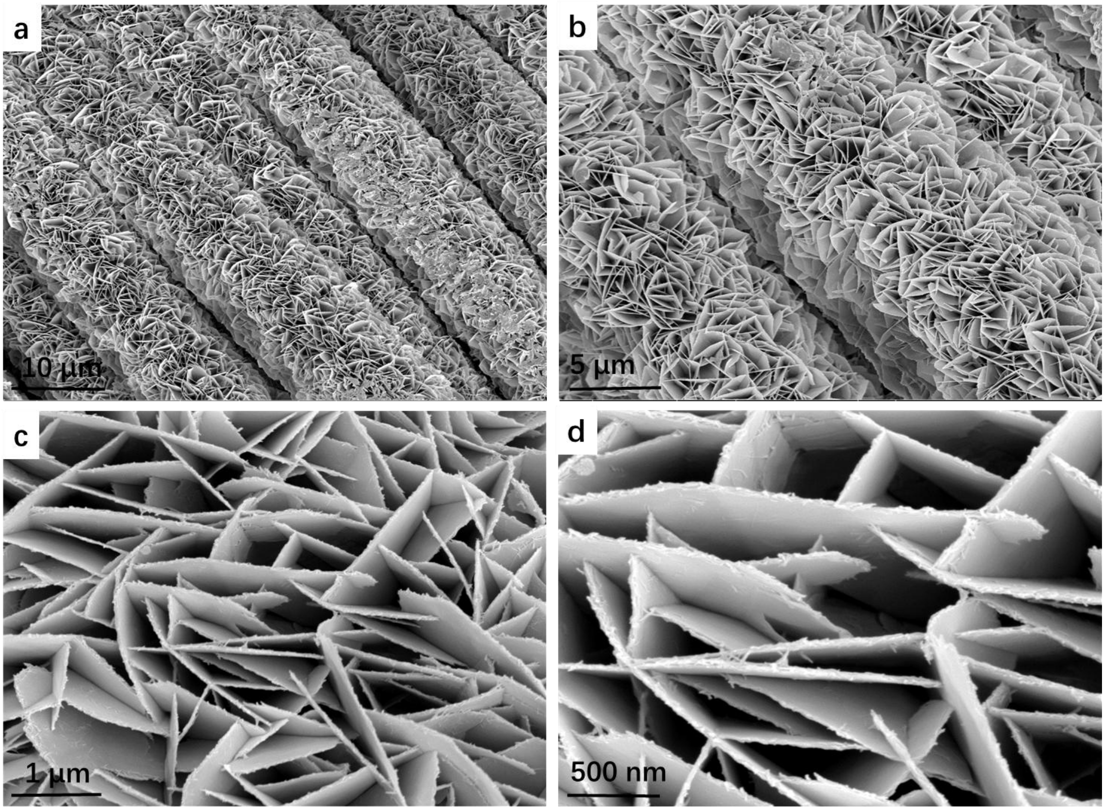

Fig. S3 SEM images of $Fe_{0.03}$-Ni LDH samples.

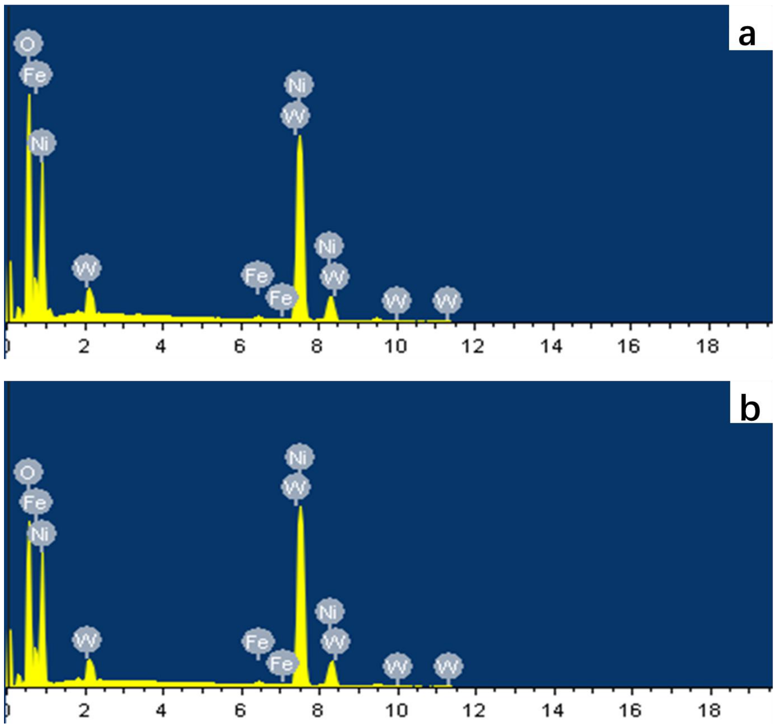

Fig. S4 EDX spectrum. a) $Fe_{0.03}W_{0.03}$-Ni LDH^B b) Post-OER $Fe_{0.03}W_{0.03}$-Ni LDH^B

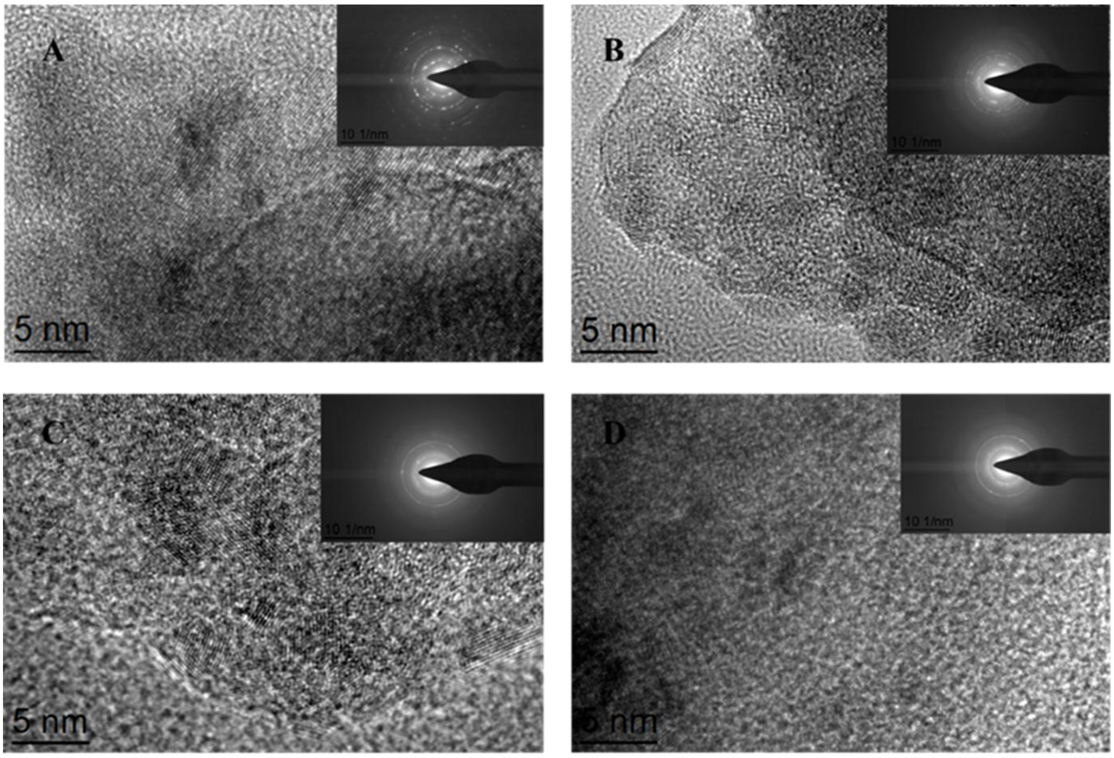

Fig. S5 (a-d) HR-TEM images of $Fe_{0.03}$ Ni LDH, $Fe_{0.03}W_{0.03}$-Ni LDH, $Fe_{0.03}W_{0.03}$-Ni LDH^{B}, post-OER $Fe_{0.03}W_{0.03}$-Ni LDH^{B} and corresponding SAED patterns (insert).

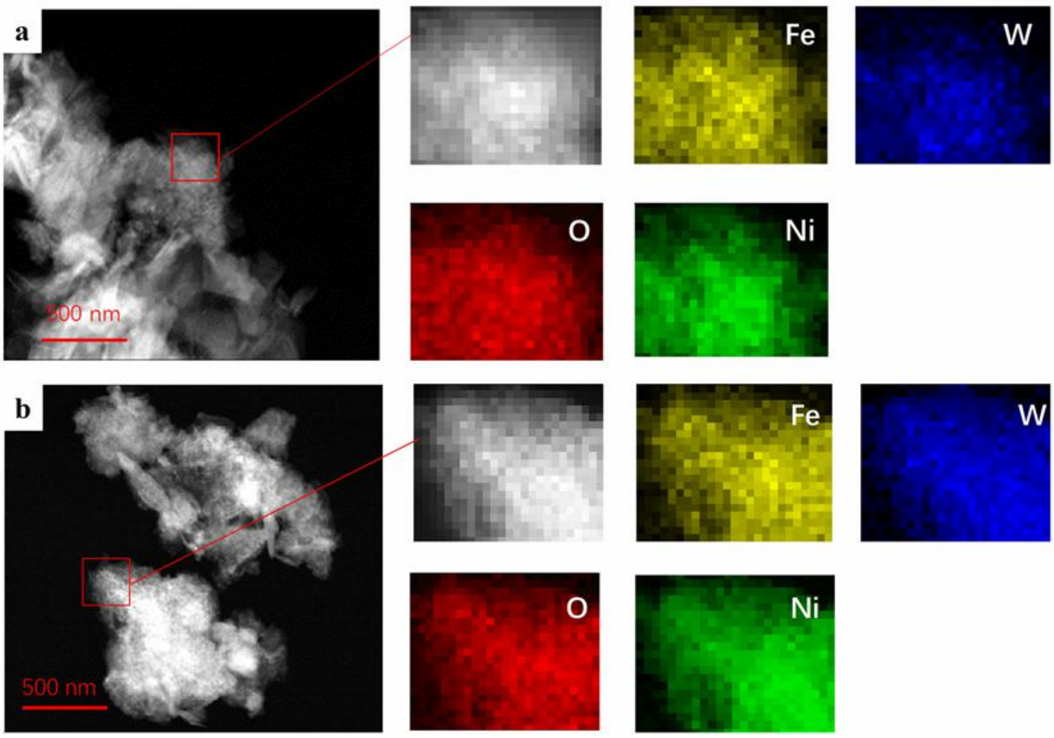

Fig. S6 Scanning transmission electron microscopy (STEM) images and the corresponding elemental mapping of Ni, Fe, W, and O. a) $Fe_{0.03}W_{0.03}$-Ni LDH; b) post-OER $Fe_{0.03}W_{0.03}$-Ni LDH^{B}.

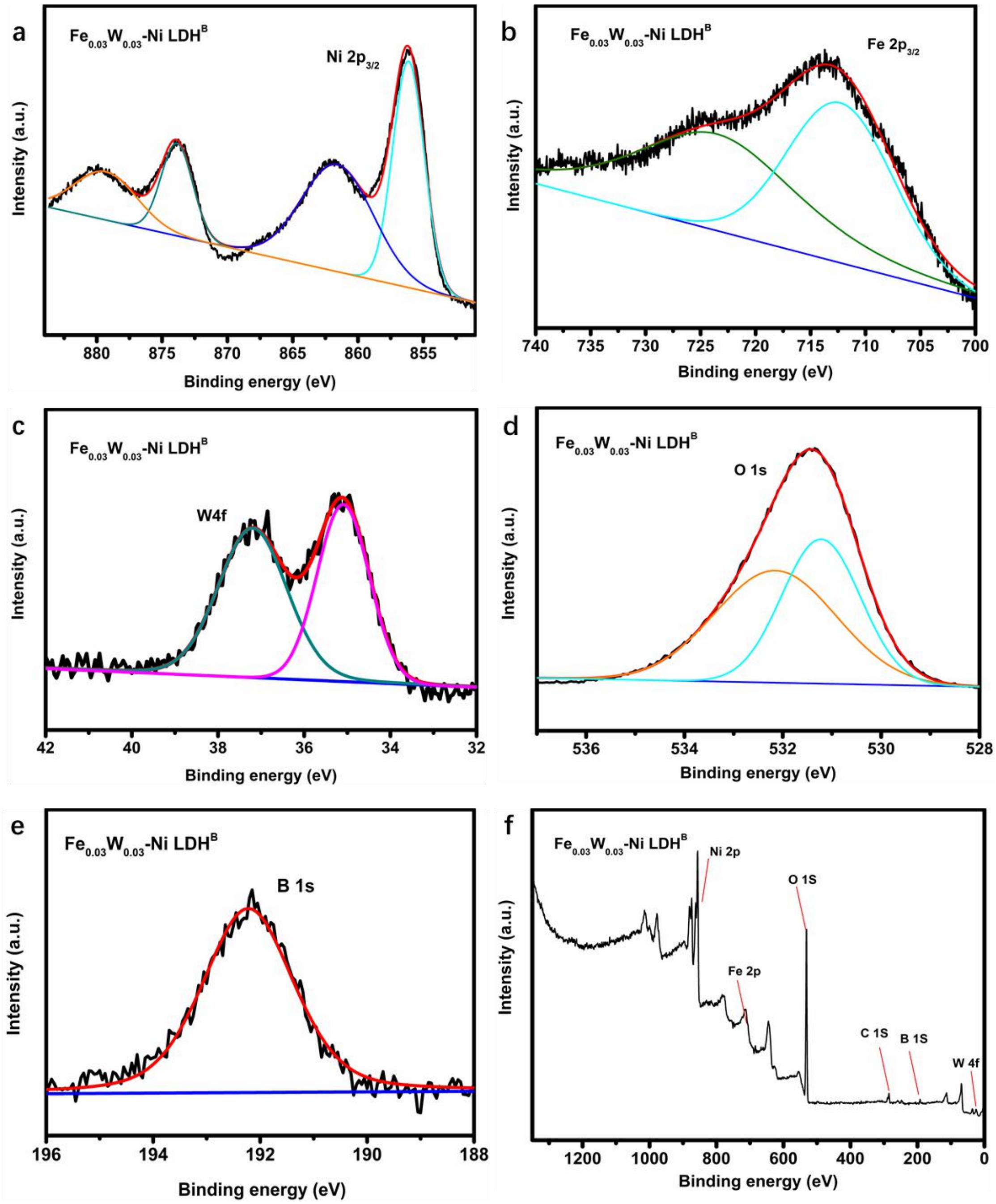

Fig. S7 a-e) XPS fine structures spectrum for $Fe_{0.03}W_{0.03}$-Ni LDH^{B} in Ni 2p, Fe 2p, W 4f, O 1s and B 1s regions. f) XPS survey spectra of $Fe_{0.03}W_{0.03}$-Ni LDH^{B}.

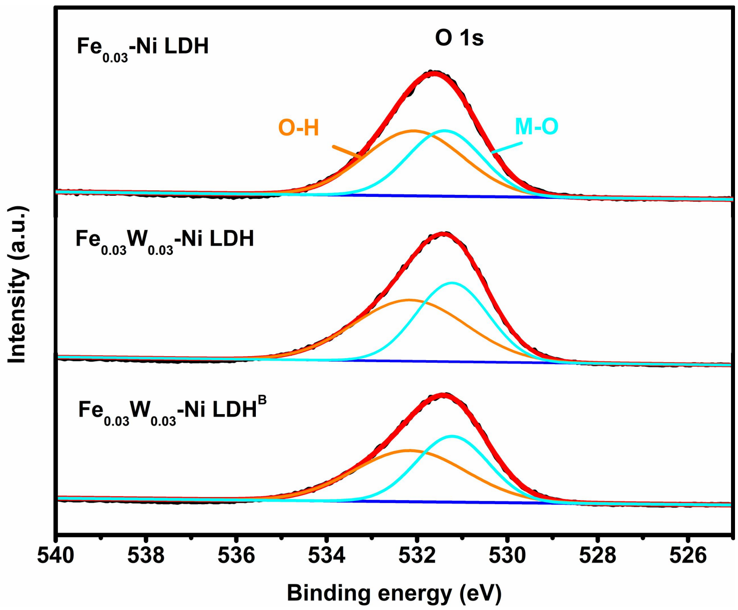

Fig. S8 XPS spectrum for $Fe_{0.03}$-Ni LDH, $Fe_{0.03}W_{0.03}$-Ni LDH and $Fe_{0.03}W_{0.03}$-Ni LDH^{B} in O1s regions.

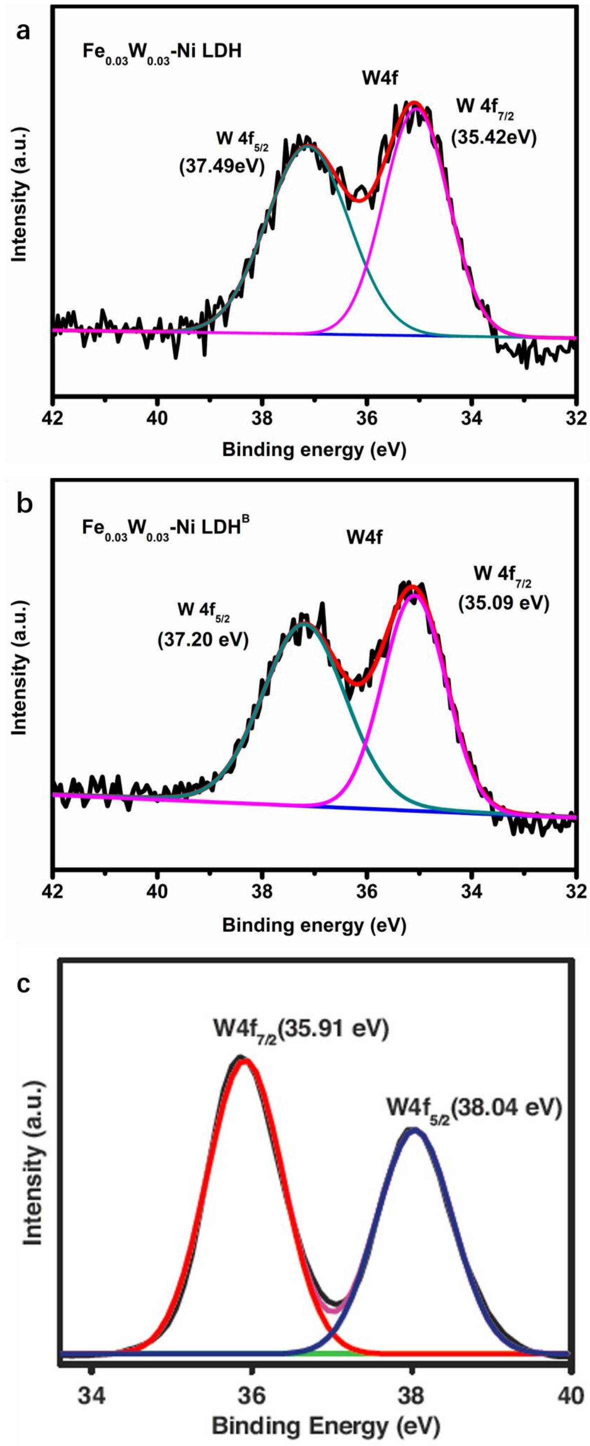

Fig. S9 XPS spectrum for a) $Fe_{0.03}W_{0.03}$-Ni LDH, b) $Fe_{0.03}W_{0.03}$-Ni LDH^{B} and c) WO_3[38] in W4f regions.

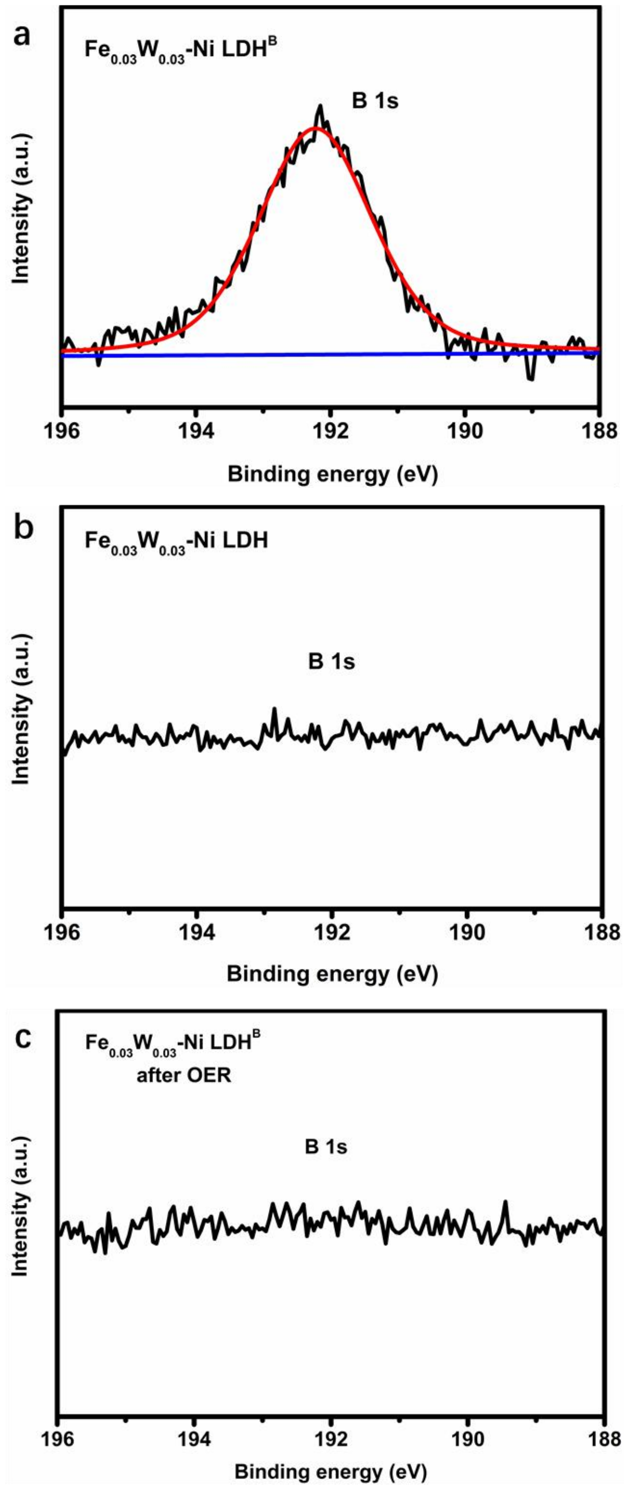

Fig. S10 XPS spectrum for a) $Fe_{0.03}W_{0.03}$-Ni LDH, b) $Fe_{0.03}W_{0.03}$-Ni LDH^B and c) $Fe_{0.03}W_{0.03}$-Ni LDH^B after OER in B1s regions.

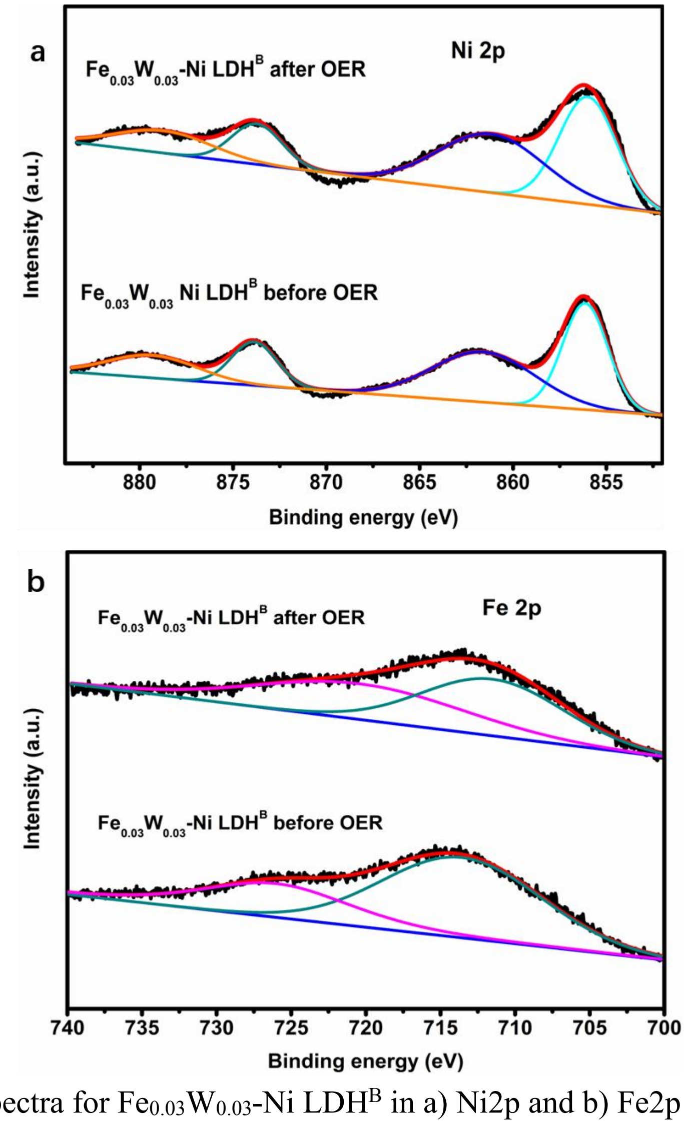

Fig. S11 XPS spectra for $Fe_{0.03}W_{0.03}$-Ni LDH^{B} in a) Ni2p and b) Fe2p regions before and after oxygen evolution reaction.

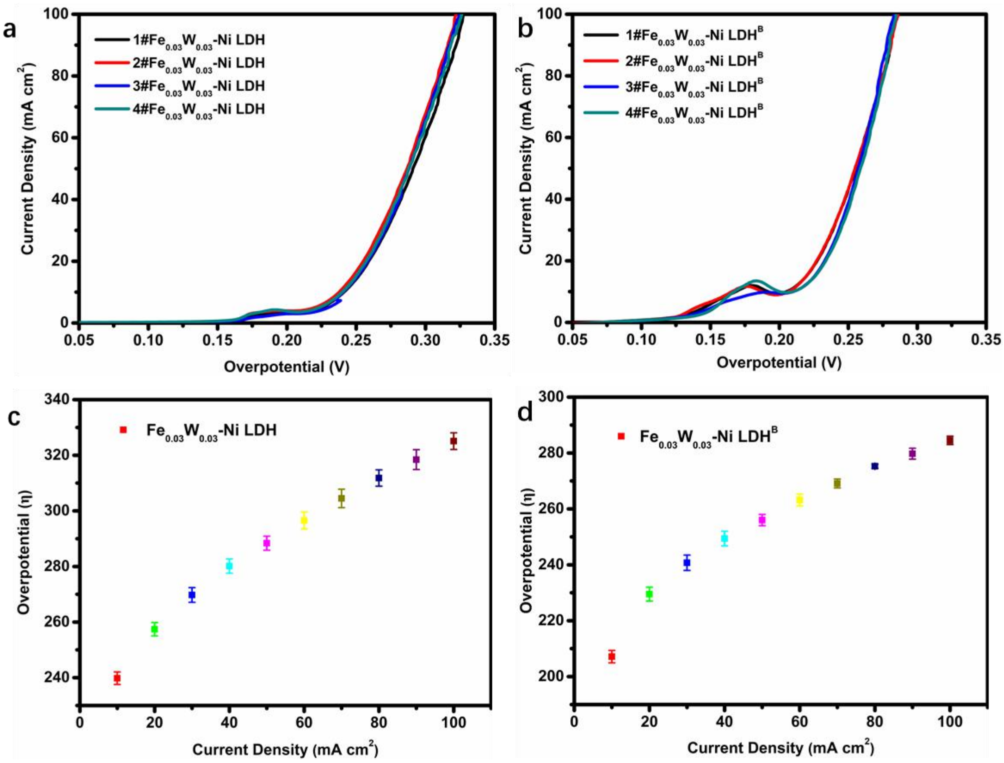

Fig. S12 Four independent OER polarization curves and scale bars of a,c) $Fe_{0.03}W_{0.03}$-Ni LDH and b,d) $Fe_{0.03}W_{0.03}$-Ni LDH^{B} catalysts on carbon clothes.

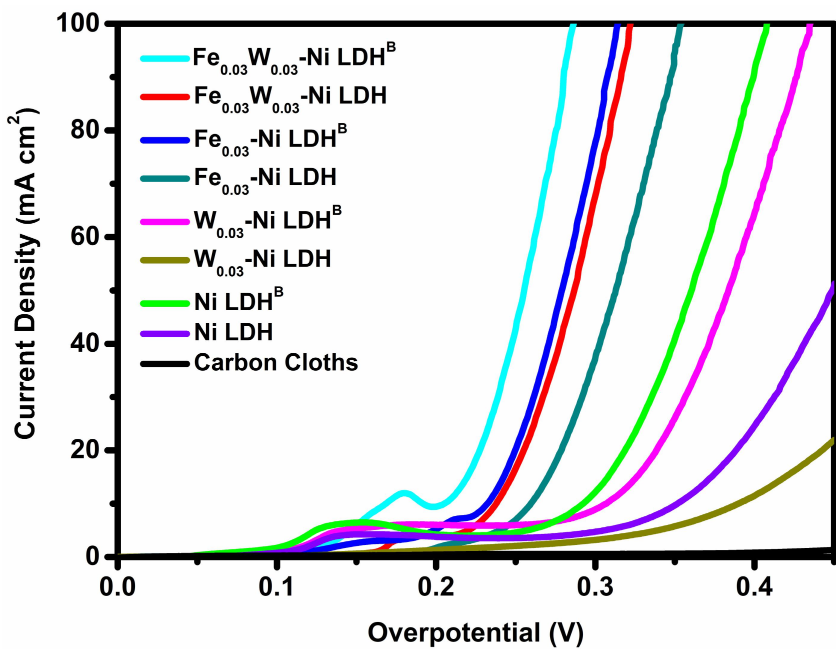

Fig. S13 LSV (Linear scan voltammetry) for more OER catalyst materials.

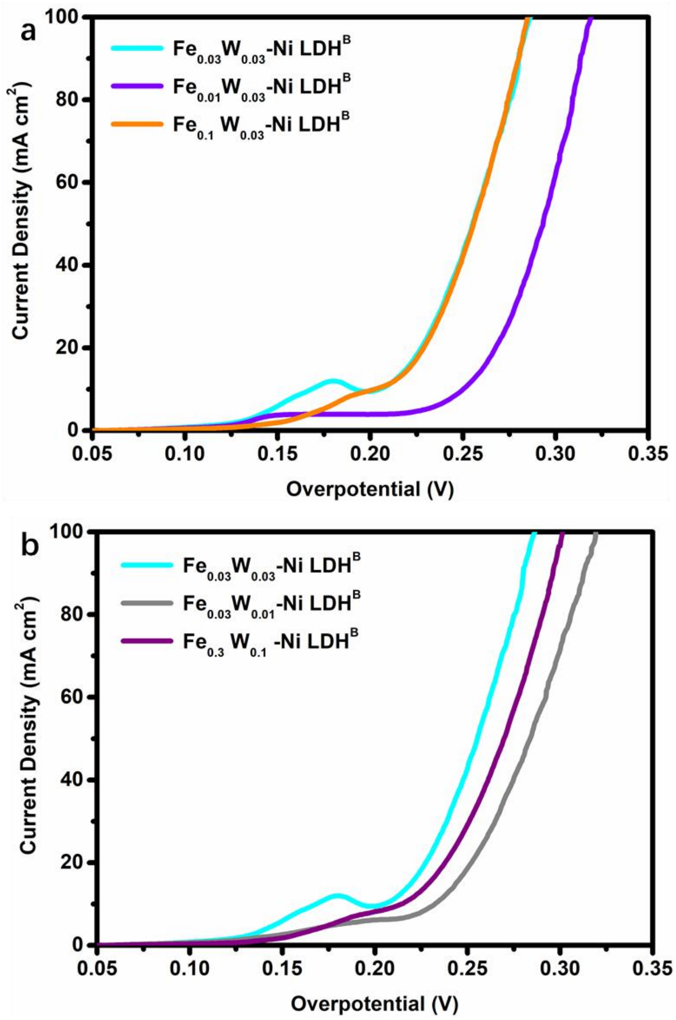

Fig. S14 a,b) LSV curves for different Fe,W atoms ratio of Fe_xW_y-Ni LDH^B OER catalyst materials.

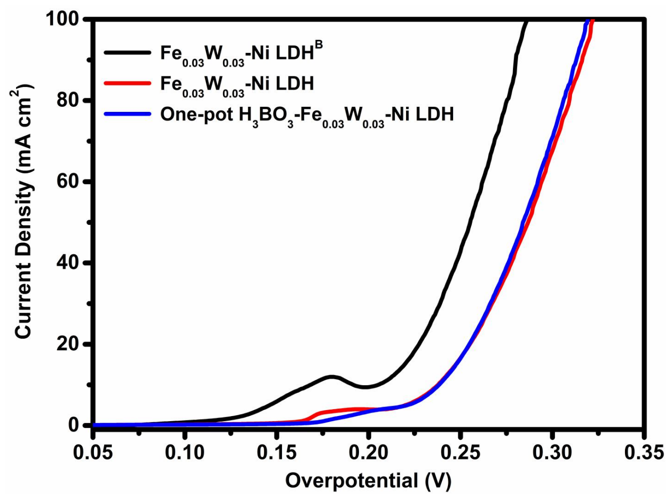

Fig. S15 LSV curves of samples doping with/without B element.

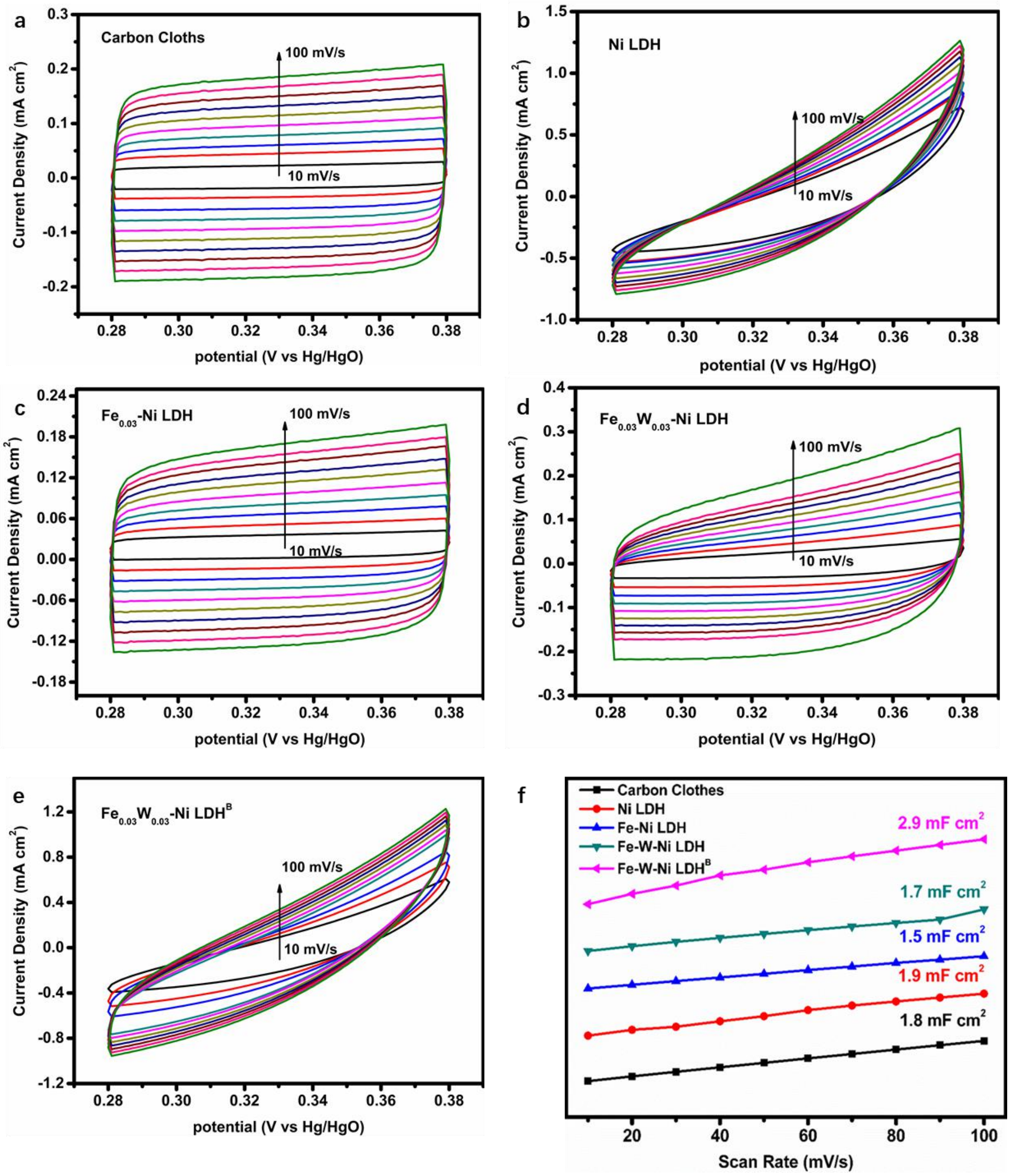

Fig. S16 a-e) Cyclic voltammograms of Carbon Clothes, Ni LDH, $Fe_{0.03}$-Ni LDH, $Fe_{0.03}W_{0.03}$-Ni LDH and $Fe_{0.03}W_{0.03}$-Ni LDH^B at scan rates from 10 to 100 mV S^{-1}. f) Double layer capacitance values (Cdl) of Carbon Clothes, Ni LDH, $Fe_{0.03}$-Ni LDH, $Fe_{0.03}W_{0.03}$-Ni LDH and $Fe_{0.03}W_{0.03}$-Ni LDH^B.

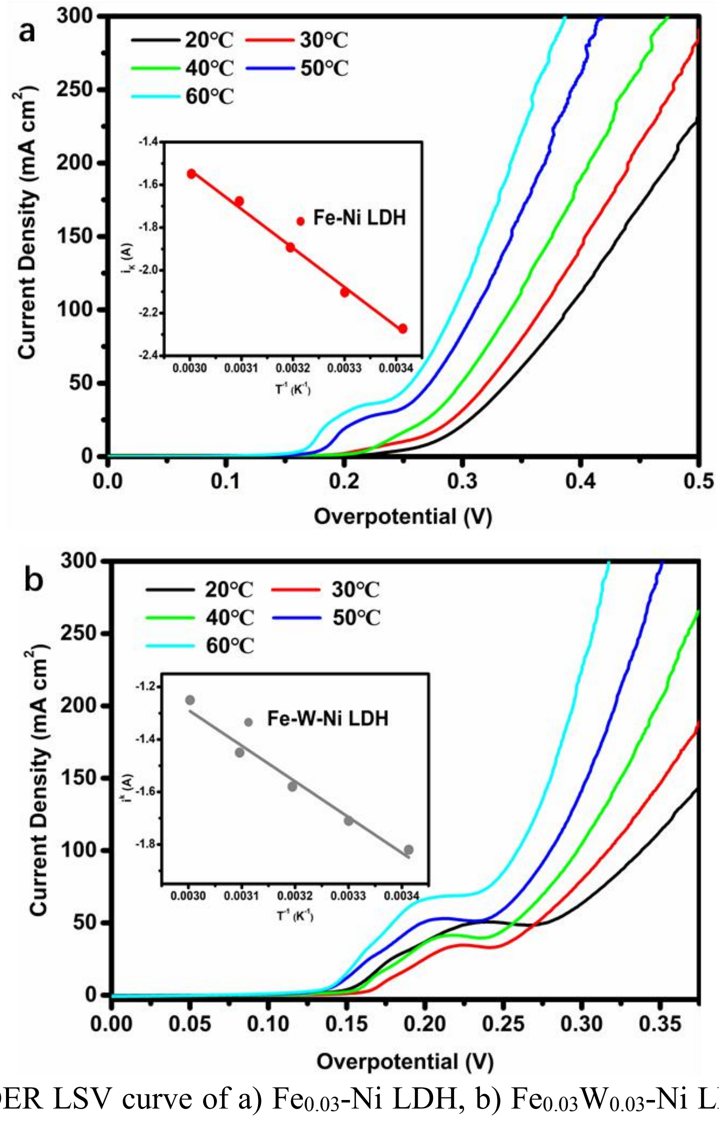

Fig. S17 The OER LSV curve of a) $Fe_{0.03}$-Ni LDH, b) $Fe_{0.03}W_{0.03}$-Ni LDH catalysts in 1 M KOH aqueous electrolyte loaded on carbon clothes with scan rate 5 mV s^{-1} at 20℃, 30℃, 40℃, 50℃ and 60℃, respectively.

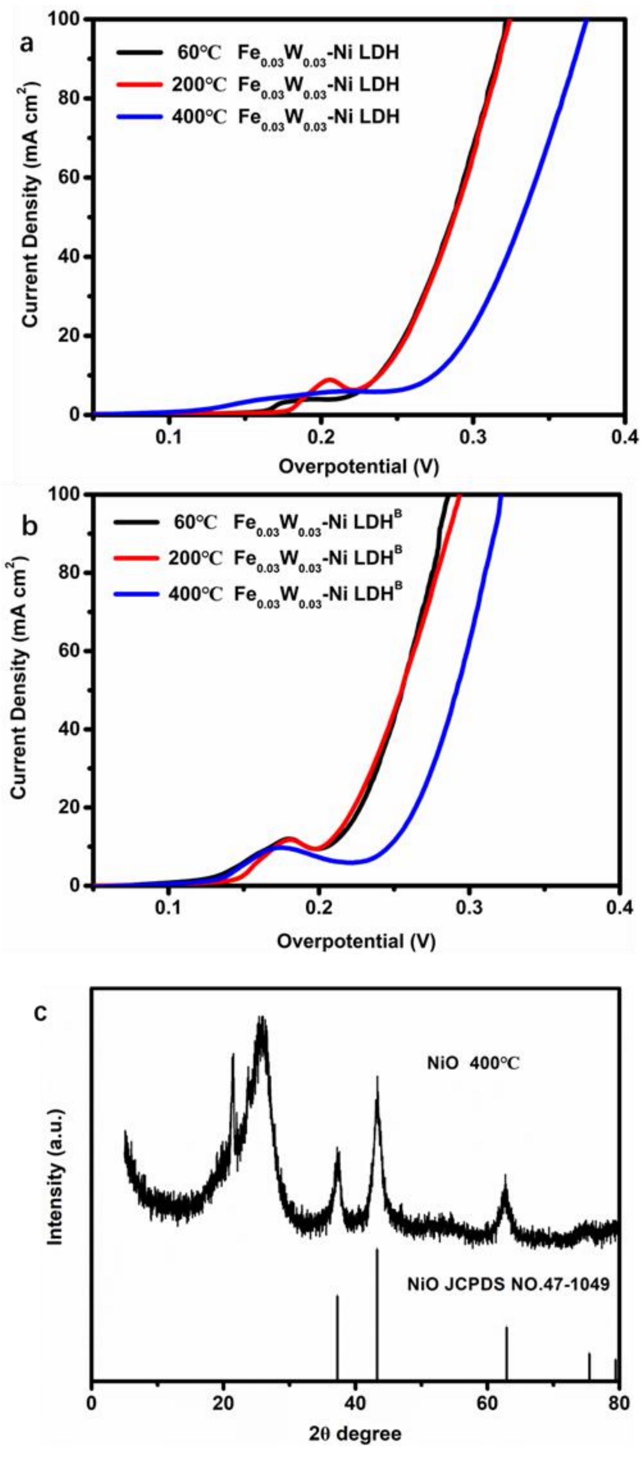

Fig. S18 a,b) LSV curves of $Fe_{0.03}W_{0.03}$-Ni LDH and $Fe_{0.03}W_{0.03}$-Ni LDH^{B} with different annealed temperature. c) XRD pattern of sample after 400°C annealed.

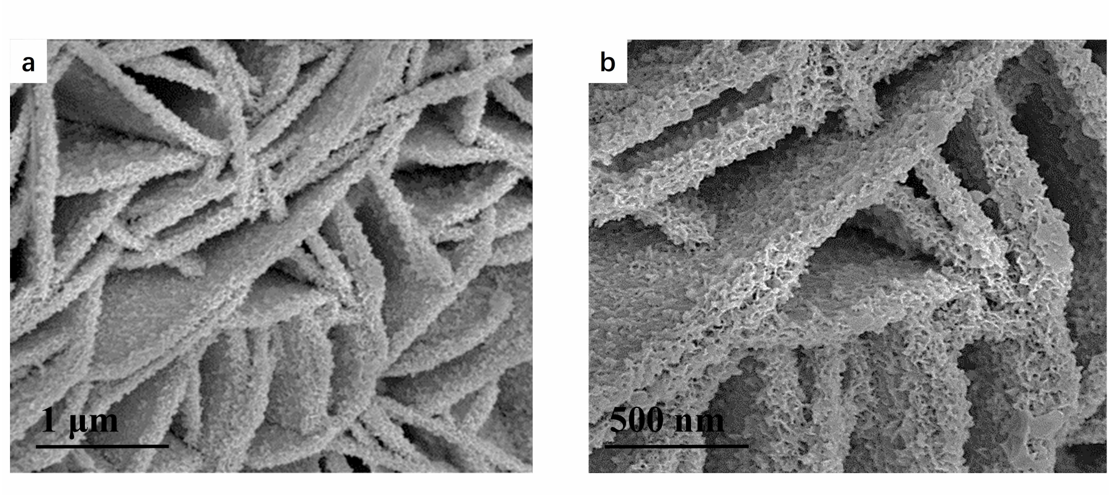

Fig. S19 a,b) SEM images of $Fe_{0.03}$-$W_{0.03}$-Ni LDH[B] samples after OER.

Table S1 ICP data of $Fe_{0.03}W_{0.03}$-Ni LDH, $Fe_{0.03}W_{0.03}$-Ni LDH[B] and $Fe_{0.03}W_{0.03}$-Ni LDH[B] after OER

materials	elements	Concentration (mg/L)	molar ratio (%)
$Fe_{0.03}W_{0.03}$-Ni LDH	Fe	3.572	3.97
	W	5.792	1.96
	Ni	88.85	94.07
$Fe_{0.03}W_{0.03}$-Ni LDH[B]	Fe	2.267	4.00
	W	4.364	2.34
	Ni	53.86	93.66
	B	4.769	--
$Fe_{0.03}W_{0.03}$-Ni LDH[B] after OER	Fe	4.99	4.62
	W	9.19	2.59
	Ni	105.3	92.79
	B	1.362	--

Table S2 Comparison of OER performance in 1.0 M KOH for $Fe_{0.03}$-$W_{0.03}$-Ni LDH[B] with other non-noble-metal electrocatalysts.

Samples	η(mV) on carbon cloth	η(mV) on nickel foam	η(mV) on gold foam	References
$Fe_{0.03}W_{0.03}$-Ni LDH[B]	205	250(50 mA cm^{-2})	—	This work
Gel-FeCoW	—	—	191	*Science* **2016**, *352*, 333.
CoFeW clusters	205	—	192	*J. Am. Chem. Soc.* **2019**, *141*, 232.
W-doped NiCoP	—	330(50 mA cm^{-2})	—	*J Mater Chem A* **2019**, *7*, 16859
Ball-milling NiFe NP	270(glassy carbon)	—	—	*Angew Chem Int Edit.* **2019**, *58*, 736.
Dry exfoliation NiFe NP	276(glassy carbon)	—	—	*Angew Chem Int Edit.* **2017**, *56,*5867.
$Fe_{0.09}Co_{0.13}$-$NiSe_2$ LDH	251	—	—	*Adv Mater.* **2018***, 30,* 1802121.
NiCoP/NiFe LDH	—	220	—	*Adv. Funct. Mater.* **2018***, 28,* 1706847.
$NaBH_4$ soaked Fe-Co_xO_y	—	204	—	*Nano Energy* **2018**, *54*, 238.